LINEAR AND NONLINEAR REFRACTIVE INDEX CHANGES IN MONOLAYER $MoSe_2$

Tran Ngoc Bich[1], Nguyen Ngoc Hieu[2,3], Ta Thi Tho[4], Le Thi Ngoc Tu[5], and Huynh Vinh Phuc[5*]

[1]Physics Department, University of Education, Hue University, Vietnam

[2]Institute of Research and Development, Duy Tan University, Vietnam

[3]Faculty of Natural Sciences, Duy Tan University, Vietnam

[4]Faculty of Mechanical Engineering, National University of Civil Engineering, Vietnam

[5]Department of Natural Sciences Teacher Education, Dong Thap University, Vietnam

[*]Corresponding author: Huynh Vinh Phuc, Email: hvphuc@dthu.edu.vn

Article history

Received: 26/01/2021; Received in revised form: 17/3/2021; Accepted: 05/4/2021

Abstract

In this work, we study the linear, the third-order nonlinear, and the total refractive index changes (RICs) caused by both intra- and inter-band transitions in monolayer $MoSe_2$ in the presence of a magnetic field by using the compact density matrix approach. The results show that RICs display the blue-shift behavior with the increase of the magnetic field. The Zeeman fields do not affect the peak positions but reduce slightly peak intensities. Besides, the strong spin-orbit coupling in monolayer $MoSe_2$ causes a significant difference in the peak due to spinning up and down. The RICs due to intra-band transition display only one peak in the THz range, while the inter-band spectra show a series of peaks in the near-infrared optical range, making monolayer $MoSe_2$ be a promising candidate for novel optoelectronic applications.

Keywords: *Magnetic field, monolayer $MoSe_2$, refractive index changes.*

ĐỘ THAY ĐỔI CHIẾT SUẤT TUYẾN TÍNH VÀ PHI TUYẾN TRONG $MoSe_2$ ĐƠN LỚP

Trần Ngọc Bích[1], Nguyễn Ngọc Hiếu[2,3], Tạ Thị Thơ[4], Lê Thị Ngọc Tú[5] và Huỳnh Vĩnh Phúc[5*]

[1] Khoa Vật lý, Trường Đại học Sư phạm, Đại học Huế, Việt Nam

[2]Viện nghiên cứu và phát triển, Trường Đại học Duy Tân, Việt Nam

[3]Khoa Khoa học Tự nhiên, Trường Đại học Duy Tân, Việt Nam

[4]Khoa Cơ khí Xây Dựng, Trường Đại học Xây dựng, Việt Nam

[5]Khoa Sư phạm Khoa học tự nhiên, Trường Đại học Đồng Tháp, Việt Nam

[*]Tác giả liên hệ: Huỳnh Vĩnh Phúc, Email: hvphuc@dthu.edu.vn

Lịch sử bài báo

Ngày nhận: 26/01/2021; Ngày nhận chỉnh sửa: 17/3/2021; Duyệt đăng: 05/4/2021

Tóm tắt

Trong công trình này, sử dụng phương pháp ma trận mật độ tối thiểu, chúng tôi nghiên cứu các số hạng tuyến tính, phi tuyến bậc ba và số hạng tổng của độ thay đổi chiết suất (RICs) do quá trình dịch chuyển nội vùng và liên vùng trong $MoSe_2$ đơn lớp khi có mặt từ trường. Kết quả cho thấy rằng khi từ trường tăng lên thì phổ RICs dịch chuyển về phía năng lượng cao. Các trường Zeeman không ảnh hưởng đến vị trí nhưng làm giảm nhẹ cường độ của đỉnh RICs. Bên cạnh đó, tương tác spin-quỹ đạo mạnh trong $MoSe_2$ đơn lớp ảnh hưởng đáng kể đến các đỉnh gây nên bởi spin hướng lên và spin hướng xuống. Phổ RICs do dịch chuyển nội vùng nằm trong vùng THz trong khi phổ RICs do dịch chuyển liên vùng nằm trong vùng hồng ngoại gần. Với các tính chất quang thú vị của mình $MoSe_2$ được hứa hẹn là một ứng viên tiềm năng cho các ứng dụng vào các thiết bị quang điện tử.

Từ khóa: *Từ trường, $MoSe_2$ đơn lớp, độ thay đổi chiết suất.*

DOI: https://doi.org/10.52714/dthu.10.5.2021.892

Cite: Tran, N. B., Nguyen, N. H., Ta, T. T., Le, T. N. T., & Huynh, V. P. (2021). Linear and nonlinear refractive index changes in monolayer $MoSe_2$. *Dong Thap University Journal of Science, 10*(5), 25-30. https://doi.org/10.52714/dthu.10.5.2021.892.

1. Introduction

Molybdenum diselenide ($MoSe_2$) is an inorganic compound of Molybdenum (Mo) and selenium (Se) (Eftekhari, 2017), an interesting member of the Transition Metal Dichalcogenides (TMDCs) family (Kormányos et al., 2014; Hien et al., 2020). In the bulk form, the semiconducting $MoSe_2$ has an indirect bandgap, but it transfers to a direct bandgap in a monolayer layer. Besides, like other TMDCs materials, $MoSe_2$ has a strong spin-orbit coupling (SOC). This makes $MoSe_2$ possessing remarkable electronic and optical properties (Wang et al., 2012), and become a potential candidate for novel optoelectronic applications (Eda & Maier, 2013).

The refractive index changes have been studied widely in the quantum well (Yildirim & Tomak 2006) and in the layered materials (Nguyen et al., 2017; Nguyen et al., 2018; Huong et al., 2020). Yildirim and Tomak studied the linear and nonlinear changes in the refractive index of a GaAs Pöschl-Teller quantum well. Their results showed that the term as a consequence of the asymmetry of the potential in the expression for the nonlinear change is found to contribute negligible values to the nonlinear refractive index in comparison to the symmetry one (Yildirim & Tomak, 2006). On studying the linear and nonlinear magneto-optical properties of monolayer phosphorene, Nguyen et al. found that the RICs in phosphorene are strongly influenced by the magnetic field. Besides, their peaks appear in two different regimes: the microwave to THz and the visible frequency. The amplitude of intra-band transition peaks is larger than that of the inter-band transitions. The resonant peaks are blue-shifted with the magnetic field (Nguyen et al., 2017). Similar results have also been observed in the monolayer MoS_2 (Nguyen et al., 2018) and monolayer WS_2 (Huong et al., 2020). Accordingly, the RICs can be used as a useful tool to study the optical properties of the layered two-dimensional material such as $MoSe_2$.

In this work, we study the linear, third-order nonlinear, and total refractive index changes (RICs) in monolayer $MoSe_2$ in a perpendicular magnetic field, using the expression in terms of single-particle eigenfunctions and eigenvalues of this material in the presence of the magnetic field. Using the density matrix theory, we calculate the RICs for both intra and inter-band transitions between the two bands. The effect of the magnetic, electric, and Zeeman fields on the RICs spectrum have been investigated quantitatively.

2. Eigenfunctions and eigenvalues of the electron in monolayer $MoSe_2$

We consider a $MoSe_2$ sheet oriented in the *(xy)* plane. When a uniform static magnetic field *B* is applied to the *z*-direction, the low-energy Hamiltonian of the system is given as follows (Hien *et al.*, 2020)

$$H_0 = v_F(\tau\sigma_x\pi_x + \sigma_y\pi_y) + (\Delta_{\tau,s} + d\Delta_z)\sigma_z + O_{\tau,s} + sM_s - \tau M_v, \quad (1)$$

where v_F is the Fermi velocity, $\tau = \pm 1$ refers to the valley index (for K and K'), $s = \pm 1$ is for spinning up/down, σ_i denotes the Pauli matrices $(i = x, y, z)$, $2d$ is the distance between the Mo and Se sublattices, $\Delta_z = eE_z$ with E_z being the electric field applied to the *z*-direction, $\vec{\pi} = \vec{p} + e\vec{A}$ is the canonical momentum with $\vec{p}$ and $\vec{A}$ being the normal momentum and the vector potential, respectively. The Dirac mass and the offset energy expressions are (Catarina *et al.*, 2019)

$$\Delta_{\tau,s} = \Delta + s\tau(\lambda_c - \lambda_v)/4, \quad (2)$$

$$O_{\tau,s} = s\tau(\lambda_c + \lambda_v)/4. \quad (3)$$

Here, $\Delta = 0.74$ eV is the intrinsic band-gap (Xiao *et al.*, 2012), the Zeeman fields are $M_i = g_i \mu_B B/2$, with $i = s, v$ corresponding to the spin and valley ones, μ_B is the Bohr magneton, and $g_i = 2 + g_i^{'}$ with $g_s^{'} = 0.29$ and $g_v^{'} = 3.03$ are the Landé factors (Kormányos et al., 2014). The corresponding eigenvalues of the Hamiltonian shown in Eq. (1) have been presented by Hien *et al.* as follows (Hien et al., 2020)

$$E_\lambda = E_{n,s}^{\tau,p} = pE_{n,s}^{\tau} + P_{\tau,s} + sM_s - \tau M_v. \quad (4)$$

Here $p = \pm 1$ refers to the conduction and valence bands, and

$$E_{n,s}^{\tau} = \sqrt{n(\hbar\omega_c)^2 + (\Delta_{\tau,s}^{z})^2}, n = 0,1,2,... \quad (5)$$

Here, $\Delta_{\tau,s}^{z} = \Delta_{\tau,s} + d\Delta_z$ and $\omega_c = v_F \sqrt{2eB/\hbar}$ is the cyclotron frequency. The eigenfunctions are $|\lambda\rangle = e^{ik_y y}\psi_{n,s}^{\tau,p}(x)/\sqrt{L_y}$ (Hien et al., 2020), where

$$\psi_{n,s}^{\tau,p}(x) = \begin{pmatrix} \tau A_{n,s}^{\tau,p}\phi_{n-1}(x-x_0) \\ B_{n,s}^{\tau,p}\phi_n(x-x_0) \end{pmatrix}, \quad (6)$$

with $\phi_n(x)$ are the normalization oscillator functions centered at $x_0 = \alpha_c^2 k_y$. The normalization constants are

$$A_{n,s}^{\tau,p} = \sqrt{\frac{pE_{n,s}^{\tau} + \Delta_{\tau,s}^{z}}{2pE_{n,s}^{\tau}}},\ B_{n,s}^{\tau,p} = \sqrt{\frac{pE_{n,s}^{\tau} - \Delta_{\tau,s}^{z}}{2pE_{n,s}^{\tau}}}. \quad (7)$$

In the next subsection, we will use above equations to evaluate the RICs.

3. The refractive index changes

To obtain the expressions for the RICs we need the expressions of the corresponding susceptibilities, using the compact density matrix approach, the linear and nonlinear optical susceptibilities for transitions between the two bands $|\lambda\rangle$ and $|\lambda'\rangle$ to be calculated as follows (Huong et al., 2020)

$$\varepsilon_0 \chi_{xx}^{(1)}(\Omega) = \frac{1}{2\pi h \alpha_c^2} \sum_{\lambda,\lambda'} \frac{(f_\lambda - f_{\lambda'})(d_{\lambda'\lambda}^{x})^* d_{\lambda'\lambda}^{x}}{E_{\lambda'\lambda} - \hbar\Omega - i\hbar\gamma_0} \quad (8)$$

$$\varepsilon_0 \chi_{xx}^{(3)}(\Omega) = -\frac{1}{2\pi h \alpha_c^2} \sum_{\lambda,\lambda'} \frac{(f_\lambda - f_{\lambda'})(d_{\lambda'\lambda}^{x})^* d_{\lambda'\lambda}^{x}}{E_{\lambda'\lambda} - \hbar\Omega - i\hbar\gamma_0} \times \left[\frac{4(d_{\lambda'\lambda}^{x})^* d_{\lambda'\lambda}^{x}}{(E_{\lambda'\lambda} - \hbar\Omega)^2 + (\hbar\gamma_0)^2} - \frac{(d_{\lambda'\lambda'}^{x} - d_{\lambda\lambda}^{x})^2}{(E_{\lambda'\lambda} - i\hbar\gamma)(E_{\lambda'\lambda} - \hbar\Omega - i\hbar\gamma_0)} \right], \quad (9)$$

where $h = 3.35\,\text{A}^0$ is the thickness of the monolayer $MoSe_2$ (Ding et al., 2011), $\alpha_c = (\hbar/eB)^{1/2}$ is the magnetic length, $d_{\lambda'\lambda}^{x} = -e\delta_{k_y,k_y}\langle\psi_{n',s'}^{\tau',p'}|x|\psi_{n,s}^{\tau,p}\rangle$ is the dipole matrix element in the x-direction, $E_{\lambda'\lambda} = E_{\lambda'} - E_\lambda$ is the energy separation, $\hbar\gamma_0 = 0.2\sqrt{B}$ (meV) (Huong et al., 2020), and $\hbar\Omega$ is the absorbed photon energy. From the expressions for the optical susceptibilities shown in Eqs. (8) and (9), we can find the RICs as follows (Rezaei et al., 2010)

$$\frac{\Delta n(\Omega, I)}{n_r} = \frac{\Delta n^{(1)}(\Omega)}{n_r} + \frac{\Delta n^{(3)}(\Omega, I)}{n_r}, \quad (10)$$

$$\frac{\Delta n^{(k)}(\Omega, I)}{n_r} = \text{Re}\left[\frac{\chi_{xx}^{(k)}(\Omega)\tilde{E}^{(k-1)}}{2n_r^2}\right], \quad (11)$$

where k = 1, 3 are for the linear and nonlinear terms, respectively, $I = 2\varepsilon_0 n_r c|\tilde{E}|^2$ is the intensity of the incident light with c = 3 x 10^8 m/s being the speed of the light and n_r = 4.25 is the refractive index of the $MoSe_2$ (Liu et al., 2014).

4. Numerical results and discussion

In this section, we will evaluate numerically the linear, the third-order nonlinear, and the total RICs in monolayer $MoSe_2$. The values of the parameters are displayed as they appear. The intensity of the light is I = 3 x 10^6 W/m^2.

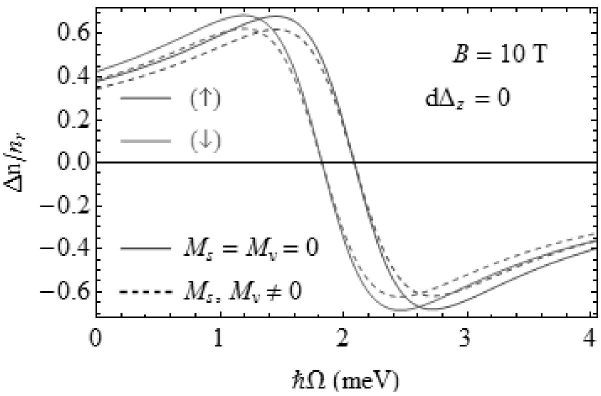

Figure 1. The linear RICs for intra-band transition is shown as a function of the photon energy at certain values of B and dΔz, for spin-up and spin-down cases

In Figure 1, the dependence of the linear RICs due to the intra-band transition on the photon energy is presented, including the effect of the spin and valley Zeeman fields. It exists only one absorption peak for each case of the spin. This result is in good agreement with that obtained in monolayer MoS_2 (Nguyen et al., 2018), WS_2 (Huong et al., 2020), and phosphorene (Nguyen *et al.*, 2017). Because the SOC in monolayer $MoSe_2$ is strong, the peak positions due to spinning up and down are separated clearly with higher energy for the up-spinning case, but there is no difference between their intensities. Besides, the Zeeman field does not affect the peak positions but reduces their intensities. This result is also in agreement with that obtained in monolayer WS_2 (Huong et al., 2020).

The effect of the electric field on the linear RICs in monolayer $MoSe_2$ is presented in Figure 2. When the electric field is taken into account, the intra-band transition RICs spectrum shifts towards the lower energy region and also reduces their intensities.

The dependence of the linear, third-order nonlinear, and the total RICs caused by the intra-band transitions on the photon energy is shown in Figure 3 at certain values of *B* and $d\Delta_z$. Since the nonlinear terms have the opposite sign in comparison to the linear ones, their contributions reduce the intensities of the total RICs. This is in good agreement with that reported in the conventional semiconductors (Yildirim & Tomak, 2006) as well as in other layered two-dimensional materials (Nguyen et al., 2017; Nguyen et al., 2018; Huong et al., 2020). Since the behavior of the RICs for up- and down-spinning cases are almost the same, in the following, we only evaluate the RICs for the up-spinning case but the results could be also validated for the down one.

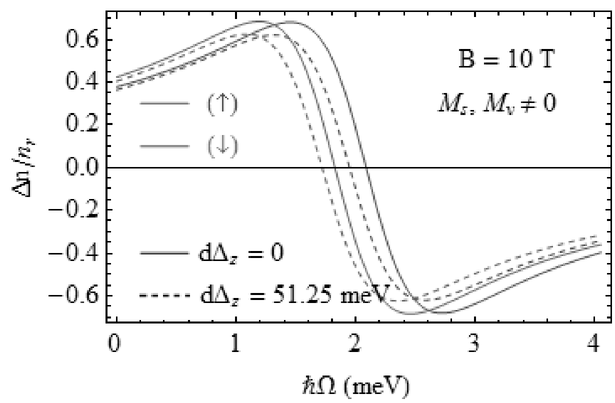

Figure 2. The linear RICs for intra-band transition including Zeeman fields are shown as a function of the photon energy at certain values of B and two different values of dΔz, for spin-up and spin-down cases

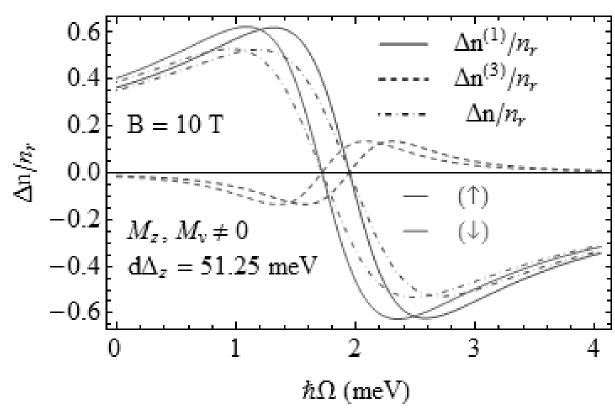

Figure 3. The linear, third-order nonlinear, and the total RICs for intra-band transition including Zeeman fields are shown as a function of the photon energy at *B* = 10 T, $d\Delta_z$ = 51.25 meV, and for spin-up and spin-down cases

In Figure 4, we depict the dependence of the linear, the third-order nonlinear, and the total RICs on the photon energy for several values of the magnetic field. The results are evaluated for the up-spinning case, including the spin and valley Zeeman fields, and at $d\Delta_z$ = 51.25 meV. It can be seen that when the magnetic field increases, the RICs spectrum shifts towards the higher region of the energy (blue-shift) and slightly reduces its intensity. This result is in good agreement with that reported in monolayer MoS_2 (Nguyen et al., 2018), WS_2 (Huong et al., 2020), and phosphorene (Nguyen et al., 2017). The blue-shift behavior of the RICs spectrum can be explained by the increase of the cyclotron energy when the magnetic field increases.

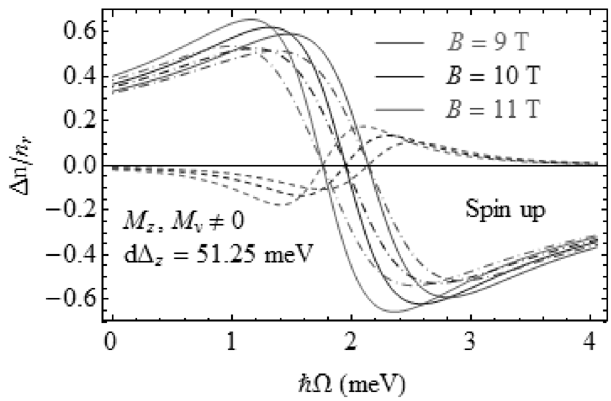

Figure 4. The linear, third-order nonlinear, and the total RICs for intra-band transition including Zeeman fields are shown as a function of the photon energy at different values of *B*, $d\Delta_z$ = 51.25 meV, and for spin-up only. The solid, dashed, and dashed-dotted lines are for the linear, the third-order nonlinear, and the total RICs, respectively

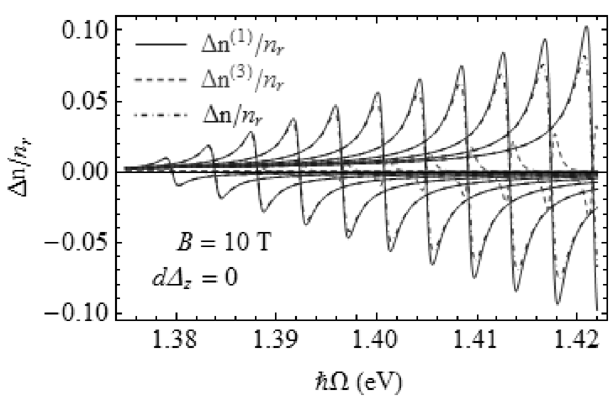

Figure 5. The linear, third-order nonlinear, and the total RICs for inter-band transition including Zeeman fields are shown as a function of the photon energy at certain values of *B*, and $d\Delta_z$, and for spin-up only

In Figure 5, we present the dependence of the linear, the third-order nonlinear, and the total RICs for the inter-band transition on the photon energy. The results are evaluated for certain values of *B*, and $d\Delta_z$ including Zeeman fields (i.e. M_s, $M_v \neq 0$). Unlike in the intra-band transiton cases, here we can see that the RICs due to the inter-band transition appear in a series of peaks at the near-infrared optical region with their intensities increase when the Landau Level increases, being in agreement with those reported in other layered two-dimensional materials (Nguyen et al., 2017; Nguyen et al., 2018; Huong et al., 2020).

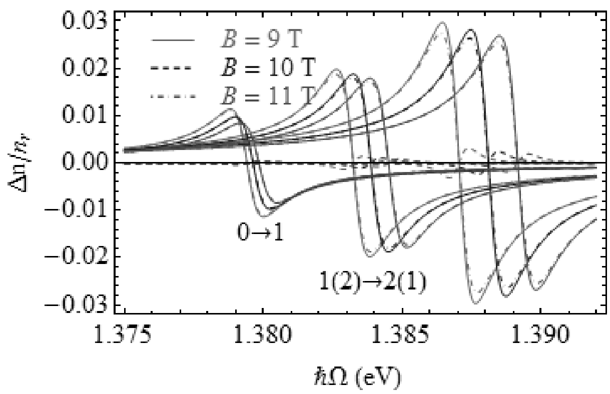

Figure 6. The linear, third-order nonlinear, and the total RICs for inter-band transition including Zeeman fields are shown as a function of the photon energy at different values of *B*, $d\Delta_z$ = 0, and for spin-up only. The solid, dashed, and dashed-dotted lines are for the linear, the third-order nonlinear, and the total RICs, respectively

Figure 6 shows the variation of the RICs due to inter-band transition with the photon energy for different values of the magnetic field. Like the case of the intra-band transition (see Figure 4), here we also see that the increase of the magnetic field shifts the peaks of the RICs spectrum to the higher energy region as the result of an increase in the cyclotron energy when the magnetic field is enhanced.

5. Conclusions

We have studied the linear, the third-order nonlinear, and the total RICs in monolayer $MoSe_2$ in the presence of a perpendicular magnetic field. The numerical results are evaluated including the combined effect of the electric and the Zeeman fields. With the strong SOC, the RICs spectrum in monolayer $MoSe_2$ depends strongly on the spinning orientation of electron: the peak positions due to the up-spinning are located at the right-hand side of that due to the down-spinning one. The effect of the electric field on the RICs spectrum for the intra-band and the inter-band transitions is opposite. Meanwhile, the effects of the magnetic field are the same in both these two types of transitions. When the magnetic field increases, the peak positions in both intra- and inter-transitions always shift to the higher energy region. These interesting optical properties make monolayer WS_2 to be a potential candidate for useful application in optoelectronic devices.

References

Catarina, G., Have J., Fernández-Rossier, J. & Peres, N. M. (2019). Optical orientation with linearly polarized light in transition metal dichalcogenides. *Physical Review B, 99*(12), 125405.1-17.

Ding, Y., Wang, Y., Ni J., Shi, L., Shi, S. & Tang, W. (2011). First principles study of structural, vibrational and electronic properties of graphene-like MX_2 (M= Mo, Nb, W, Ta; X= S, Se, Te) monolayers. *Physica B: Condensed Matter, 406*(11), 2254-2260.

Eda, G. & Maier, S. A. (2013). Two-dimensional crystals: managing light for optoelectronics. *ACS Nano, 7*(7), 5660-5665.

Eftekhari, A. (2017). Molybdenum diselenide (MoSe2) for energy storage, catalysis, and optoelectronics. *Applied Materials Today, 8*, 1-17.

Hien, N. D., Nguyen, C. V., Hieu, N. N., Kubakaddi, S., Duque C., Mora-Ramos, M., Dinh, L., Bich, T. N. & Phuc, H. V. (2020). Magneto-optical transport properties of monolayer transition metal dichalcogenides. *Physical Review B, 101*(4), 045424.1-13.

Huong, P. T., Muoi, D., Bich, T. N., Phuc, H. V., Duque, C. A., Nguyen, P. T. N., Nguyen, C. V., Hieu, N. N. & Hoa, L. T. (2020). Intra-and inter-band magneto-optical absorption in monolayer WS_2. *Physica E: Low-dimensional Systems and Nanostructures, 124*, 114315.1-6.

Kormányos, A., Zólyomi, V., Drummond, N. D. & Burkard, G. (2014). Spin-orbit coupling, quantum dots, and qubits in monolayer transition metal dichalcogenides. *Physical Revview X, 4*(1), 011034.1-16.

Liu, H.-L., Shen, C.-C., Su, S.-H., Hsu, C.-L., Li, M.-Y. & Li, L.-J. (2014). Optical properties of monolayer transition metal dichalcogenides probed by spectroscopic ellipsometry. *Applied Physics Letters, 105*(20), 201905.1-4.

Nguyen, C. V., Hieu, N. N., Duque, C. A., Khoa, D. Q., Hieu, N. V., Tung, L. V. & Phuc, H. V. (2017). Linear and nonlinear magneto-optical properties of monolayer phosphorene. *Journal of Applied Physics, 121*(4), 045107.1-6.

Nguyen, C. V., Hieu, N. N., Muoi, D., Duque, C. A., Feddi, E., Nguyen, H. V., Phuong, L. T., Hoi, B. D. & Phuc, H. V. (2018). Linear and nonlinear magneto-optical properties of monolayer MoS_2. *Journal of Applied Physics, 123*(3), 034301.1-7.

Rezaei, G., Karimi, M. & Keshavarz, A. (2010). Excitonic effects on the nonlinear intersubband optical properties of a semi-parabolic one-dimensional quantum dot. *Physica E: Low-dimensional Systems and Nanostructures, 43*(1), 475-481.

Wang, Q. H., Kalantar-Zadeh, K., Kis, A., Coleman, J. N. & Strano, M. S. (2012). Electronics & optoelectronics of two-dimensional transition metal dichalcogenides. *Nature nanotechnology, 7*(11), 699-712.

Xiao, D., Liu, G.-B., Feng, W., Xu X. & Yao, W. (2012). Coupled Spin and Valley Physics in Monolayers of MoS_2 and Other Group-VI Dichalcogenides. *Physical Review Letters, 108*(19), 196802.1-5.

Yildirim, H. & Tomak, M. (2006). Intensity-dependent refractive index of a Pöschl-Teller quantum well. *Journal of Applied Physics, 99*(9), 093103.1-5.